Journal of Inflammation Research

Dovepress

Open Access Full Text Article

ORIGINAL RESEARCH

Analysis of the Potential Link Between Dermatomyositis and Cancer

Jianwei Guo[1,2,*], Tianyi Lei[1,3,*], Xiang Yu[1,3], Peng Wang[1,2], Hongyuan Xie[1,3], Guilin Jian[1,4], Quanbo Zhang[1,2,*], Yufeng Qing[1,3]

[1]Research Center of Hyperuricemia and Gout, Affiliated Hospital of North Sichuan Medical College, Nanchong, 637000, People's Republic of China; [2]Department of Geriatrics, Affiliated Hospital of North Sichuan Medical College, Nanchong, 637000, People's Republic of China; [3]Department of Rheumatology and Immunology, Affiliated Hospital of North Sichuan Medical College, Nanchong, 637000, People's Republic of China; [4]Emergency Department,Suining Third People, S Hospital, Suining, Sichuan, 629000, People's Republic of China

*These authors contributed equally to this work

Correspondence: Quanbo Zhang; Yufeng Qing, Email quanbozhang@126.com; qingyufengqq@163.com

Background: Dermatomyositis (DM) is an inflammatory muscle disease that increases the risk of cancer, although the precise connection is not fully understood. The aim of this study was to investigate the mechanisms linking DM to cancer and identify potential therapeutic targets.

Methods: We conducted differential gene expression analysis on the GSE128470 dataset and employed WGCNA to pinpoint key genes related to DM. Central genes were identified with the LASSO and SVM-RFE methods. The expression levels and diagnostic relevance of these genes were confirmed via the GSE1551 dataset. Immune cell infiltration was analyzed in relation to central genes, and RT–qPCR was utilized to evaluate the expression of key genes across various cancers.

Results: In total, differentially expressed genes (DEGs), involved mainly in innate immunity, cytokine responses, and autoimmune diseases, were identified. In the WGCNA, 399 significant genes related to DM were identified, with central genes including MIF, C1QA, and CDKN1A. Immune infiltration analysis revealed diverse immune cell populations in DM patients, with significant correlations between central genes and these immune cells. MIF levels were notably elevated in various tumors and correlated with the prognosis of specific cancers. Furthermore, MIF was negatively associated with most immune cells but positively correlated with CD4+ Th1 cells, NKT cells, and MDSCs. Factors such as immune regulatory elements, TMB, and MSI indicated that MIF may affect immunotherapy outcomes. The increased expression of MIF mRNA was confirmed via RT–qPCR.

Conclusion: The findings demonstrate that MIF, C1QA, and CDKN1A are differentially expressed in DM patients, with MIF showing significant alterations in DM patients with cancer. MIF may serve as a crucial prognostic biomarker and therapeutic target for various cancers, playing a pivotal role in linking DM to cancer through the modulation of CD4+ Th1 cells, NKT cells, and MDSCs.

Keywords: dermatomyositis, pan-cancer, immune infiltration, machine learning, WGCNA, MIF

Introduction

Dermatomyositis (DM) is an unexplained inflammatory myopathy that is clinically characterized by skin lesions and skeletal muscle inflammation[1] and often involves different organ systems, such as muscles, blood vessels, joints, the esophagus and lungs.[2] There are two different forms of DM, namely, juvenile and adult DM (aDM). The prevalence of aDM is estimated to be 5–10 per million people per year, and twice as many women as men have the condition.[3] The etiology of DM is unclear, and genetic, environmental and immune mechanisms are thought to be associated with susceptibility and morbidity.[4,5] Cancer is a complex disease involving the interaction of tumors with the immune system.[6] An increasing number of studies have shown that DM is a paraneoplastic autoimmune disease. Approximately 25% of DM cases are associated with malignant tumors.[7,8] Potentially malignant tumors frequently occur in the lung, stomach, pancreas, cervix, ovary, breast, or bladder, and lymphoma is common.[9–12] Nasopharyngeal cancers are also common in Asian Americans,[13] and the risk of malignancy increases with age.[14,15]

Received: 26 July 2024
Accepted: 27 November 2024
Published: 3 December 2024

Cancer development is a complex and multifactorial process. Immune components within tumors, known as the tumor immune microenvironment (TIME), have long been associated with tumor development, recurrence and metastasis.[16] These include congenital immune cells (macrophages, neutrophils, mast cells, myeloid-derived suppressor cells (MDSCs), dendritic cells and natural killer cells) and adaptive immune cells (T and B lymphocytes), as well as cancer cells and their surrounding matrix (fibroblasts, endothelial cells, pericytes and stromal cells).[17] These different cells control and shape tumor progression through direct contact or the production of cytokines and chemokines that communicate with each other. The findings from a growing body of research have suggested that inflammatory responses also play a decisive role in different stages of tumor development, including initiation, promotion, malignant transformation, invasion and metastasis.[18,19] Notably, chronic and nonregressive inflammation increases the risk of cancer and is considered a marker for cancer.[20] Current research has revealed that immunity and inflammation play critical roles in tumor development. Although DM is a chronic autoimmune inflammatory disease with multiple possible cancers, the potential association between DM and human cancers has rarely been reported and deserves further investigation.

Materials and Methods

Data Set Downloading and Data Processing

The GSE128470[21] and GSE1551[22] datasets were retrieved and downloaded from the Gene Expression Omnibus (GEO, http://ncbi.nlm.nih.gov/geo). GSE128470 was used for training and included 12 DM samples and 12 healthy control (HC) samples. GSE1551 was used for validation and included 13 DM samples and 10 hC samples. The platform information between the probe ID and the gene symbol was subsequently converted according to GPL96. The probes that did not have a gene symbol were removed, and the average expression value for multiple probes that corresponded to the same gene symbol was calculated. Data on 33 cancer and normal tissues in The Cancer Genome Atlas (TCGA), including mRNA expression, mutation and clinical data, were downloaded from the UCSC Xena database (https://xenabrowser.net/data files/).

Differentially Expressed Gene (DEG) Analysis

The R software limma package was used to study the DEGs.[23] The threshold for DEGs was set to | log2 fold change (FC) | > 1 and adjustment $p < 0.05$. The dplyr, ggplot2, ggrepel, and pheatmap packages were used to create volcano plots and expression maps.

Functional Enrichment Analysis

Gene Ontology (GO) was used to identify genes, gene products and characteristic biological properties,[24] including those in the biological processes (BP), cellular components (CC) and molecular functions (MF) domains. The Kyoto Encyclopedia of Genes and Genomes (KEGG) was used to analyze gene function and related information about advanced genome function.[25] Disease occurrence was determined via disease ontology (DO) for mining high-throughput biological data.[26] The R software packages clusterProfiler, org.Hs.eg.db, DOSE, enrichplot and ggplot2 were used to visualize DEGs for GO, KEGG, and DO (adjustment $p < 0.05$ and $q < 0.05$).

Weighted Gene Coexpression Network Analysis (WGCNA)

WGCNA contributes to the study of gene set expression and is used to cluster genes or proteins into modules on the basis of interconnectedness and to calculate correlations between modules and clinical phenotypes to identify characteristic genes.[27] First, a suitable soft threshold power β is calculated to achieve scale-free topology with an R2 criterion > 0.9. The average linkage hierarchical clustering method is then used to cluster proteins into different modules labeled with different colors. Each module contains at least 50 proteins, and the threshold for module merging is set to 0.25. Pearson correlation was applied to determine the correlation between each module and DM, and modules with p values less than 0.05 and high correlation coefficients were selected for analysis. Model membership (MM) and gene significance (GS) were estimated to correlate modules with clinical characteristics, and clinically important genes with MM > 0.8 and GS > 0.2 were screened.[28] The R package WGCNA was used to perform this work.

Venn

The R software VennDiagram package was used to build Venn diagrams, and a wide range of graphical tools were used to describe the merging and intersections of multiple datasets and distinguish them.[29]

Identification of Hub Genes

Support vector machines (SVMs) are among the most important tools for machine learning and are used mainly for Class II data.[30] Among them, SVM recursive feature removal (SVM-RFE) can filter relevant features and remove relatively unimportant feature variables to achieve higher classification performance. The SVM-REF classifier was constructed via the R package e1071 and cross-validated to eliminate regression features. Least absolute shrinkage and selection operator (LASSO) is characterized by variable selection and complexity adjustment while fitting to the generalized linear model.[31] The R package glmnet was used to perform LASSO regression and obtain the lambda value of the simplest model within a range of variance for truncation (lambda.1se), which has good performance but only 10 cross-validation variables.

Receiver Operating Characteristic (ROC) Curve Analysis

The R software pROC function was used to create a receiver operating characteristic (ROC) curve to determine the area under the ROC curve (AUC) to screen feature genes and assess their diagnostic value.[32]

Immune Infiltration Analysis

The GSVA package uses a single sample gene pooling analysis (ssGSEA) algorithm to assess the immunological characteristics of each sample included in the study comprehensively[33] and to analyze the different infiltration levels of various immune cells between DM patients and HCs. The ssGSEA algorithm involved 28 immune cells.[34] To analyze the associations between immune cells and hub genes, the corrplot package was used to obtain the Spearman rank correlation coefficient.

GeneMANIA

GeneMANIA (http://genemania.org) was used to analyze associated data to identify relevant genes, including protein–protein, protein–DNA and genetic interaction, pathway, response, gene and protein expression data, protein domain and phenotype screening profiles.[35] In this study, we used a database to explore the network of hub genes and their functions.

Timer 2.0

TIMER2.0 (http://timer.comp-genomics.org/) is an online website primarily based on the TCGA for a comprehensive exploration of tumor immunology and clinical and genomic features.[36] In this study, we used this tool to analyze the differential expression of hub genes across cancers and explore the correlation between MIF and immune cell infiltration across cancers.

GEPIA

GEPIA (www.gepia.cancer-pku.cn/) is an online tool based on TCGA and GTEx data that can be used to customize single-gene differential analysis.[37] In this study, the expression of MIF in tumor tissues and corresponding normal tissues was analyzed via the GEPIA database, and the data as displayed as BodyMap and dot plots. We also used this database to explore the relationship between MIF expression and tumor pathological stage. For all of the above methods, log2 (TPM + 1) was used as the logarithmic scale.

Expression of MIF and the Prognosis of Cancer Patients

Univariate regression analysis and Kaplan–Meier survival analysis were used to calculate the relationships between overall survival (OS) and MIF expression levels in 33 different types of cancer. The R survival, survminer, and forestplot packages were used to generate the plots, and the high and low expression level data were checked via the Wilcoxon test. $P < 0.05$ was considered statistically significant.

TISIDB

TISIDB (http://cis.hku.hk/TISIDB/index.php) is a portal where tumors and the immune system interact.[38] TISIDB was used to analyze the relationships between MIF expression and the expression of immunoinhibitors, immunostimulators, and MHC molecules.

Expression of MIF is Associated with the TMB and MSI Across Cancers

The tumor mutational burden (TMB) refers to the number of somatic mutations per terabyte in the coding region and is a new genetic biomarker for predicting the efficacy of immunotherapy.[39] Microsatellite instability (MSI) is defined as any change in microsatellite length during DNA replication, leading to the emergence of new microsatellite alleles.[40] TMB and MSI scores were obtained from pan-cancer datasets for Spearman correlation analysis of TMB, MSI and MIF expression levels.

Clinical Samples and Data Collection

The peripheral venous blood and clinical data of 20 patients with DM and 20 patients with DM complicated by cancer (DM+Ca) who were admitted to the Affiliated Hospital of North Sichuan Medical College from Jan 2023 to March 2024 were collected. The laboratory indicators, including the hypersensitive-c-reactive protein (hsCRP) level, erythrocyte sedimentation rate (ESR), white blood cell count (WBC), neutrophil granulocyte count (GR), lymphocyte count (LY), monocyte count (Mo), serum albumin (ALB), serum globulin (GLOB), serum uric acid (sUA), serum urea (Urea), serum creatinine (Crea), and estimated glomerular filtration rate (eGFR), were obtained from the laboratory department of the Affiliated Hospital of North Sichuan Medical College. All patients with DM met the diagnostic criteria for DM proposed by Bohan and Peter in 1975. In addition, 30 healthy people were selected as healthy controls (HCs) at the Physical Examination Center of the Affiliated Hospital of North Sichuan Medical College during the same period. All participants provided informed consent. The studies involving human participants were reviewed and approved by the Ethics Committee of the Affiliated Hospital of North Sichuan Medical College (No. 2022ER575-1) and were conducted in accordance with the ethical norms of the 1975 helsinki Declaration.

RNA Extraction and Real-Time Quantitative Polymerase Chain Reaction (RT-qPCR)

Total RNA was extracted via the TRIzol method. The synthesized complementary cDNA was cryopreserved at -80°C until qPCR was performed. The expression of MIF, C1QA and CDKN1A was measured by means of real-time qPCR via the Applied Biosystems QuantStudio™ 12K Flex Real-Time PCR system (Applied Biosystems; Thermo Fisher Scientific, Inc). The reaction mixture contained 5.2 μL of SYBR Green real-time PCR master mix (Takara Bio, Inc)., forward and reverse primers (0.3 μL each), the cDNA sample (1 μL) and double-distilled H_2O (3.4 μL). The thermocycling conditions were as follows: 95°C for 10 min. All reactions were performed in triplicate. The housekeeping gene β-actin was used as the internal control. The primer sequences are shown in Table 1.

Table 1 Real-Time Fluorescent Quantitative PCR Primers

Gene names	Forward Primer Sequence	Reverse primer Sequence
β-actin	5′-GAGCTACGAGCTGCCTGACG −3	5′-GTAGTTTCGTGGATGCCACAG −3′
MIF	5′- GCAGAACCGCTCCTACAGCAAG −3′	5′-TGGCCGCGTTCATGTCGTAATAG-3′
C1QA	5′-TCTGCACTGTACCCGGCTA −3′	5′-CCCTGGTAAATGTGACCCTTTT-3′
CDKN1A	5′-TCTGCACTGTACCCGGCTA-3′	5′-GCACAAGGGTACAAGACAGTG-3′

Statistical Analysis

Statistical analysis and graphics were performed via R software (version 4.1.2) and GraphPad Prism (version 8.0). Quantitative data with an approximately normal distribution are expressed as the means ± standard deviations, and nonnormally distributed data are expressed as the medians. Statistical analyses of clinical and laboratory indicators were compared via independent samples t tests, Mann–Whitney *U*-tests, and one-way ANOVA, followed by the least significant difference (LSD) post hoc test. The Wilcoxon test was used to calculate significance and compare the distributions of different immune cells between DM and HC samples. ROC analysis was used to evaluate the power of MIF. Univariate Cox regression analysis and Kaplan–Meier (logarithmic rank test) analysis were used to assess the prognostic role of MIF expression in each type of cancer. Spearman correlation analysis was performed to assess the statistical relationships between MIF and other factors, such as immune cell infiltration levels, immunomodulators, TMB and MSI. P values less than 0.05 were considered statistically significant.

Results

Data Analysis and DEG Identification

In total, 321 DEGs were identified via analysis of the GSE128470 dataset with limma packages, and among them, 216 DEGs were upregulated, and 105 were downregulated after adjustment ($P < 0.05$ and $|\log2\ FC| > 1$). The DEG volcanic maps (Figure 1A) and thermal maps of the first 50 DEGs (Figure 1B) are shown.

DEG Functional Analysis

GO analysis revealed that the DEGs comprised genes related to BP processes including response to viruses, negative regulation of the congenital immune response, the type I interferon signaling pathway, the signaling-mediated signaling pathway, immune regulation of the effector process, and the MDA-5 signaling pathway; CC processes including MHC complex protein, membrane raft, early endosome, and phagocytic vesicle membrane; and MF processes including double-strand RNA, cytokine binding, and peptide binding. (Figure 2A). KEGG analysis revealed that these pathways are related to the NOD-like receptor signaling pathway, RIG-I-like receptor signaling pathway, necroptosis pathway, and Toll-like receptor signaling pathway (Figure 2B). DO analysis revealed that these DEGs were associated with infection, autoimmune diseases, lymphatic diseases, hematopoietic diseases and cancer (Figure 2C).

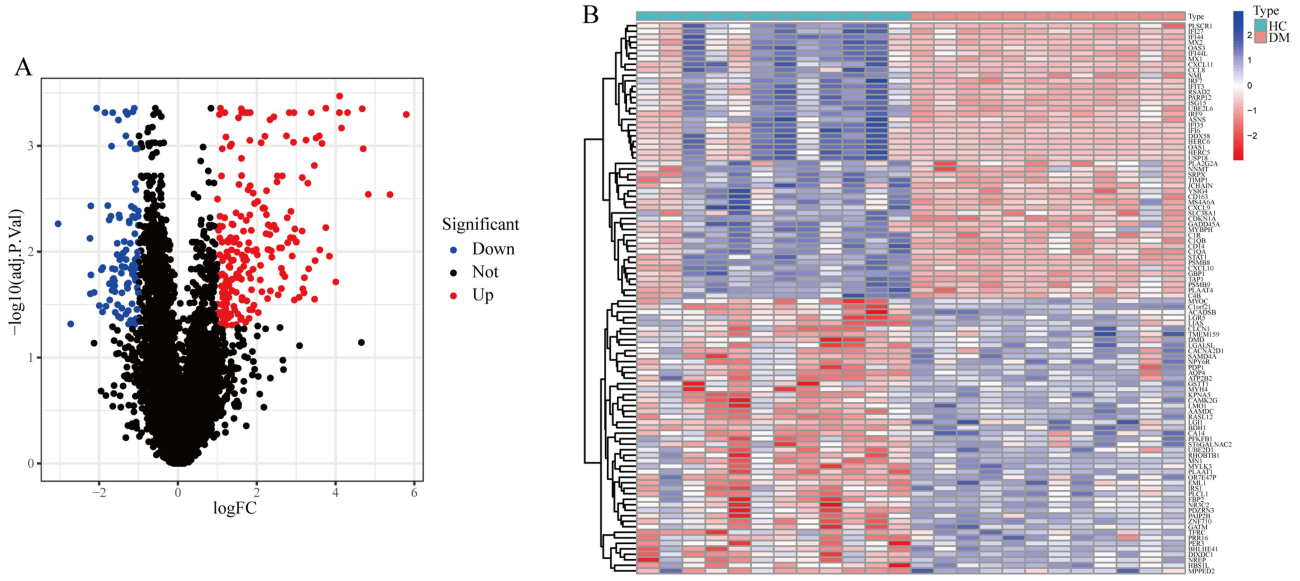

Figure 1 DEG identification. (**A**) A volcanic map of DEGs. (**B**) The top 50 thermal maps of DEGs.

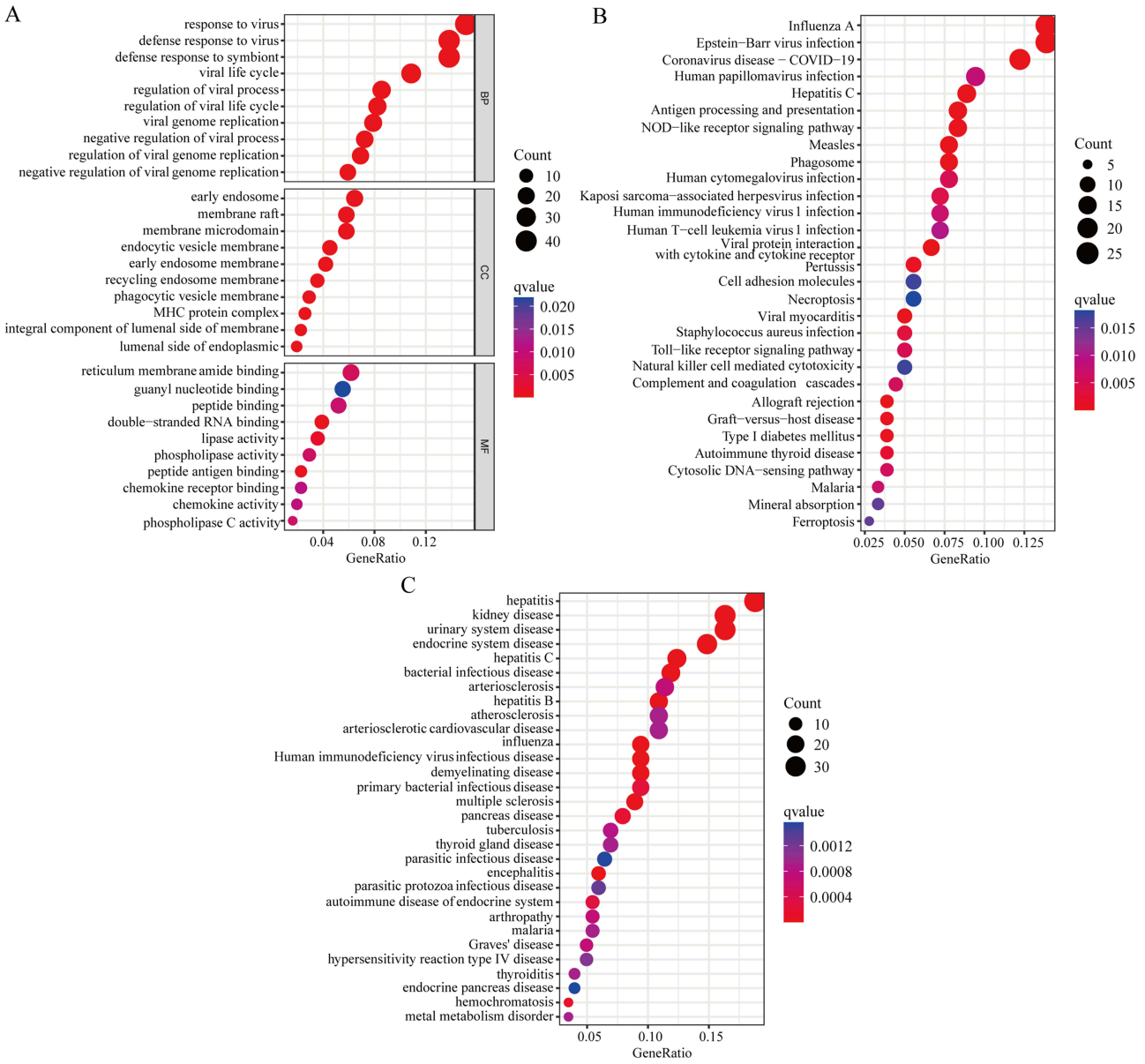

Figure 2 DEGs functional analysis. (**A**) GO analysis, where BP, CC, and MF show the top 10 enrichment results. (**B**) KEGG analysis, showing the first 30 enrichment results. (**C**) DO analysis, showing the first 30 enrichment results.

WGCNA

On the basis of the dataset GSE128470 expression matrix, we constructed a gene coexpression network via the R package WGCNA. The soft threshold was set to 9, R2 > 0.9, and the average connectivity was close to 0 (Figure 3A). After merging the strong association module with a 0.25 clustering height limit, we used the dynamic hybrid cutting method to construct a hierarchical clustering tree. Each leaf represents a gene, and each branch represents a module that aggregates all genes at similar levels of expression. Next, we summarized the functional equivalents into one large module, resulting in 15 modules (Figure 3B). Module membership (MM) indicates the correlation between module gene expression values and module feature genes (MEs). Gene salience (GS) indicates the correlation between module genes and samples. Modules were associated with clinical characteristics according to MM and GS values (Figure 3C), where dark red modules (R2 = 0.66, *P* = 9E-04), orange modules (R2 = 0.74, *P* = 7E-05), and black modules (R2 = 0.77, P = 3E-05) were defined as central modules. Among the 3 modules, the gene with high chain properties was identified as the potential essential gene most strongly associated with DM. On the basis of the truncation criteria (MM > 0.8 and GS > 0.2), 399 key genes were identified (Figure 3D).

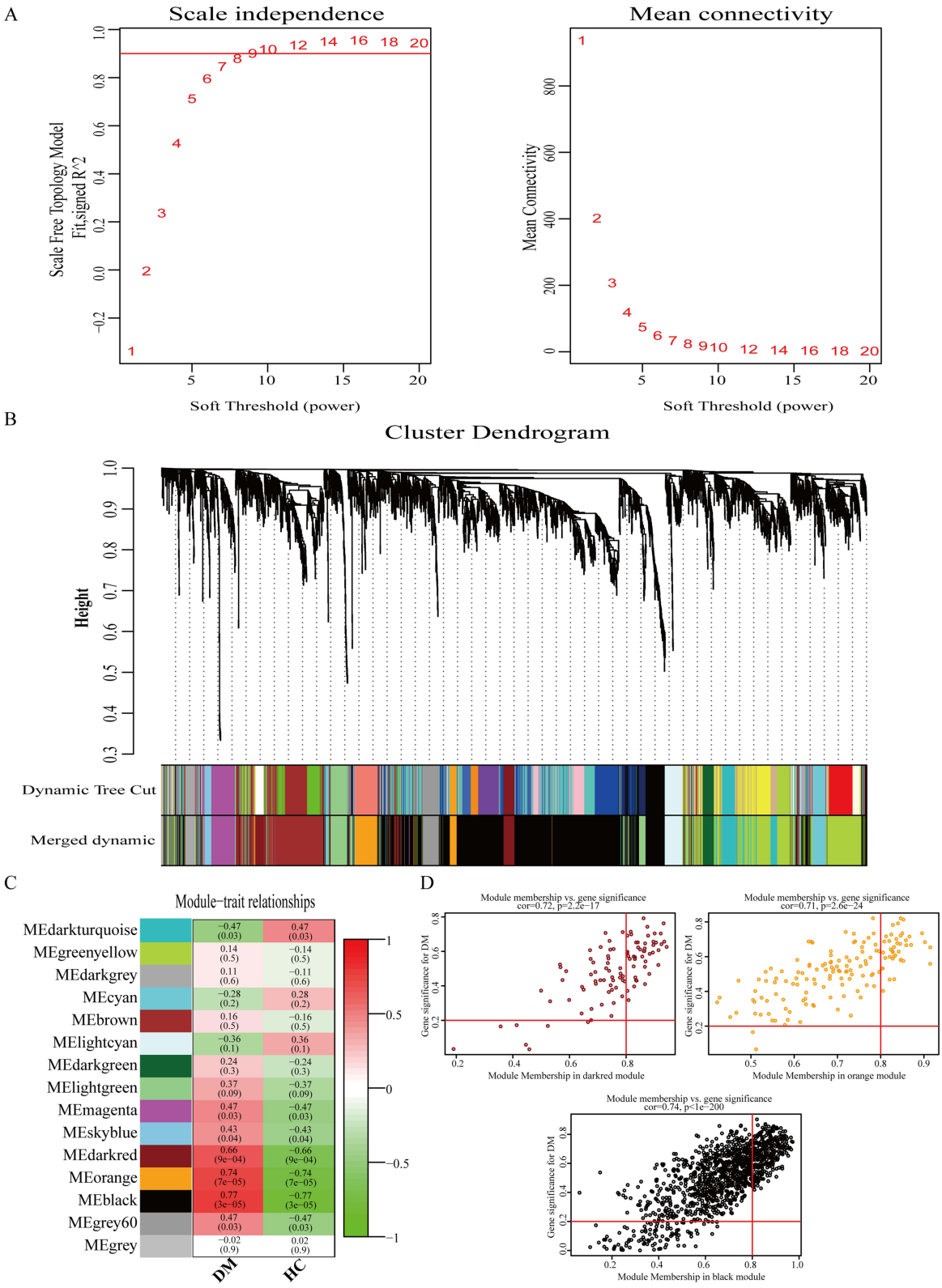

Figure 3 WGCNA. (**A**) Scale-free fit index analysis of 1–20 soft threshold power (left) and average connectivity analysis (right). (**B**) Genes are classified into modules through hierarchical clustering, with different colors representing different modules. (**C**) Thermal maps of the modular characteristics associated with DM and HC. (**D**) Scatter maps of genes in the dark red, Orange and black modules.

Identification and Verification of Hub Genes

A comparison of the DEGs and key module genes identified by WGCNA yielded 169 overlapping genes (Figure 4A). Overlapping genes were used for LASSO regression analysis, and 6 candidate genes were identified by lambda.1se (Figure 4B). In addition, SVM-REF analysis revealed that the model containing 31 genes had the best accuracy (Figure 4C). Combining the results of the two algorithms (Figure 4D), macrophage migration inhibitor (MIF), complement 1Q subcomponent A chain (C1QA) and cyclin-dependent kinase inhibitor 1A (CDKN1A) were ultimately identified as the hub genes. Then, we used the GSE128470 and GSE1551 datasets to analyze the differences in the 3 hub genes and verify the diagnostic markers. In the GSE128470 and GSE1551 datasets, MIF, C1QA and CDKN1A were highly expressed in DM (Figure 4E and F). Moreover, the ROC curve revealed high values for DM in both datasets, with AUCs greater than 0.9 (Figure 4G and H).

Single-Sample Immune Infiltration Analysis

The distribution of immune cells between DM and HC samples was determined with the ssGSEA algorithm. The results revealed that the numbers of activated CD4+ T cells, activated dendritic cells, CD56bright natural killer cells, central memory CD4+ T cells, central memory CD8+ T cells, effector memory CD4+ T cells, effector memory CD8+ T cells, gamma delta T cells, immature B cells, macrophages, MDSCs, memory B cells, natural killer T cells (NKTs), neutrophils, regulatory T cells, and type 1 T helper cells were greater in the DM patients than in the HCs, and no significant differences were found in the other immune cells (Figure 5A). Spearman analysis of MIF, C1QA, CDKN1A and immune cells revealed that MIF, C1QA, CDKN1A and these differential immune cells were highly positively correlated (Figure 5B).

Hub Gene Interaction Analysis

GeneMANIA creates a PPI network for the hub genes. MIF is involved in the intrinsic apoptotic signaling pathway, the regulation of the apoptotic signaling pathway, ligand-activated transcription factor activity, myeloid leukocyte migration, leukocyte chemotaxis, the intrinsic apoptotic signaling pathway in response to DNA damage by p53 class mediators, and the IRE1-mediated unfolded protein response, among other processes (Figure 5C). C1QA is related mainly to complement activation and the humoral immune response. CDKN1A is related to cell cycle regulation and protein kinase regulation (see Supplementary Figure S1A and S1B).

Validation of the Hub Genes in Human Peripheral Blood

The mRNA expression levels of MIF, C1QA and CDKN1A in the peripheral blood mononuclear cells of DM patients were measured via RT–qPCR, and the results revealed that the mRNA expression levels of C1QA and CDKN1A in the DM group and DM+Ca group were significantly greater than those in the HC group ($P<0.05$); however, there was no significant difference between the DM group and the DM+Ca group. Even so, there were significant differences in MIF among the three groups ($P<0.05$); MIF expression was significantly higher in the DM+Ca group than in the DM group or HC group and was higher in the DM group than in the HC group (Figure 6A-C). In addition, our analysis of the clinical data of patients in the three groups revealed that the serum ALB concentration was significantly lower in the DM+Ca group than in the DM+Ca and HC groups. We also performed a ROC analysis with tumor-related indicators and positive and negative anti-TIF1-Y antibodies as the dependent variables and MIF mRNA expression levels as the independent variables, in which MIF mRNA expression levels were diagnostically significant for CA199 positivity ($P<0.001$, AUC=0.839) and anti-TIF1-Y antibody positivity ($P=0.001$, AUC=0.806) (Figure 6D-H) (Table 2).

Expression of MIF in Human Cancer

TIMER2.0 verified the difference in the expression of MIF between tumor and normal tissues. The expression of the MIF gene was significantly upregulated in 18 types of cancer, including BLCA, BRCA, CESC, CHOL, COAD, ESCA, HNSC, KICH, KIRC, KIRP, HLIC, LUAD, LUSC, PRAD, STAD, THCA and UCEC (Figure 7A). Combining the results of GeneMANIA analysis with the high expression of MIF in most tumors, we analyzed MIF further. In addition, we used

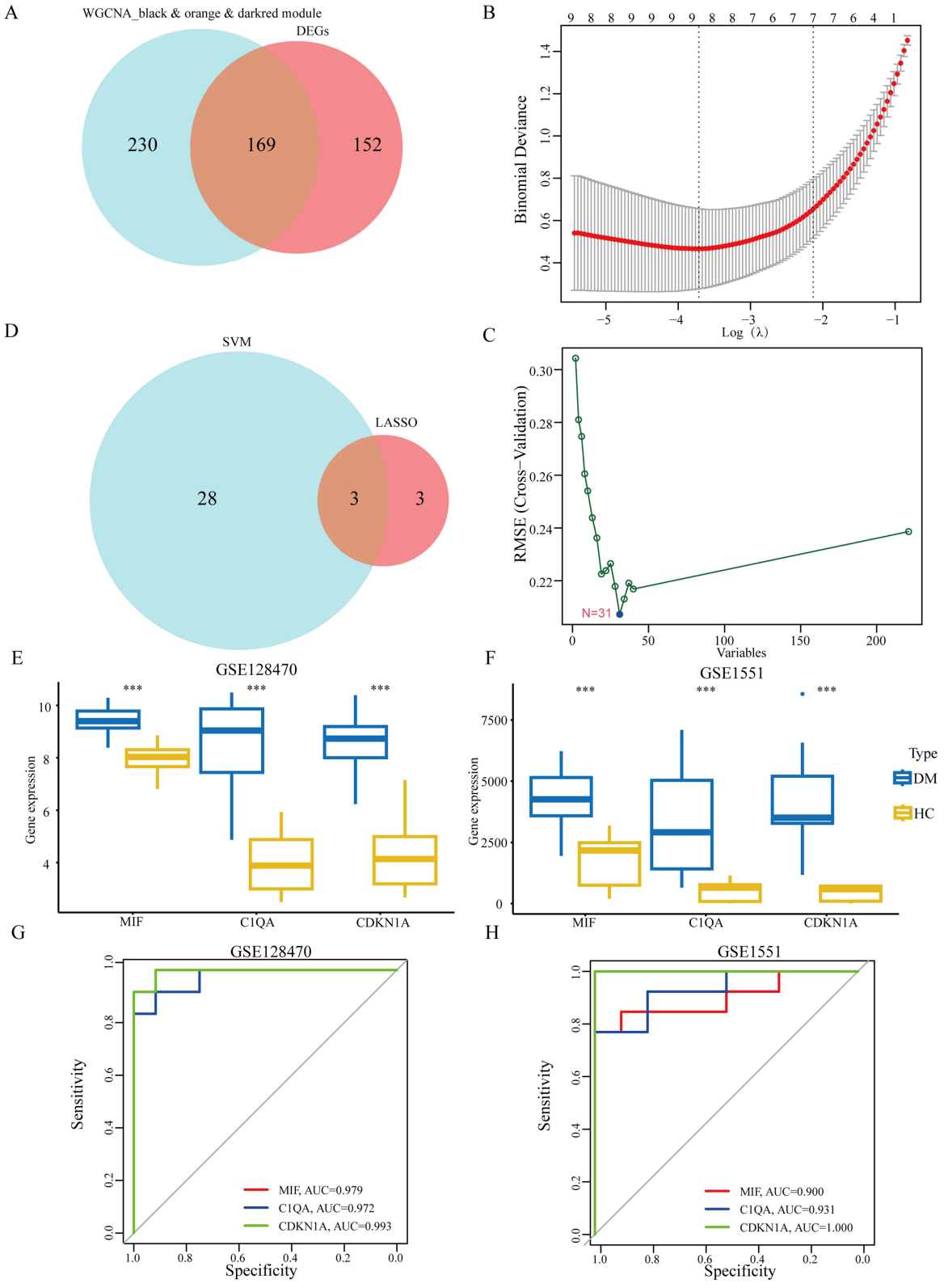

Figure 4 Identification and verification of hub gene. (**A**) cross venn diagram of WGCNA and DEGs. (**B**) Lasso analysis. (**C**) SVM-RFE analysis. (**D**) Cross venn diagram of LASSO and SVM results. (**E, F**) Differential analysis of hub gene in GSE128470 and GSE1551. (**G, H**) ROC results of hub gene in GSE128470 and GSE1551. ***P < 0.001.

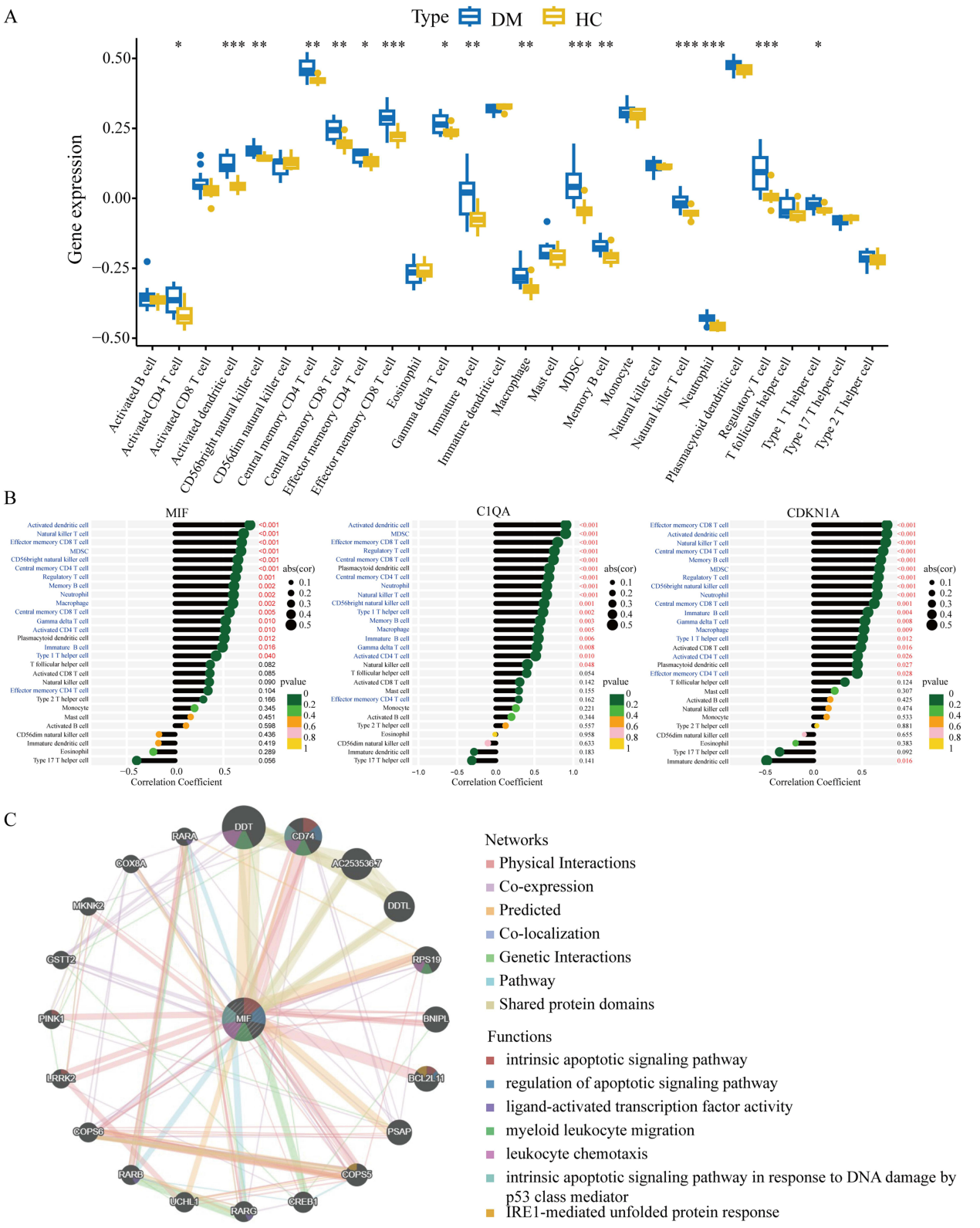

Figure 5 Immune infiltration, hub gene and immune cell correlation, hub gene PPI analysis. (**A**) Single sample GSEA immune infiltration differential analysis box, blue; dermatomyositis, yellow, healthy. * P < 0.05, ** P < 0.01, *** P < 0.001. (**B**) Correlation analysis between MIF, C1QA, CDKN1A and immune cells. (**C**) The PPI network of MIF and its functional analysis come from GeneMANIA.

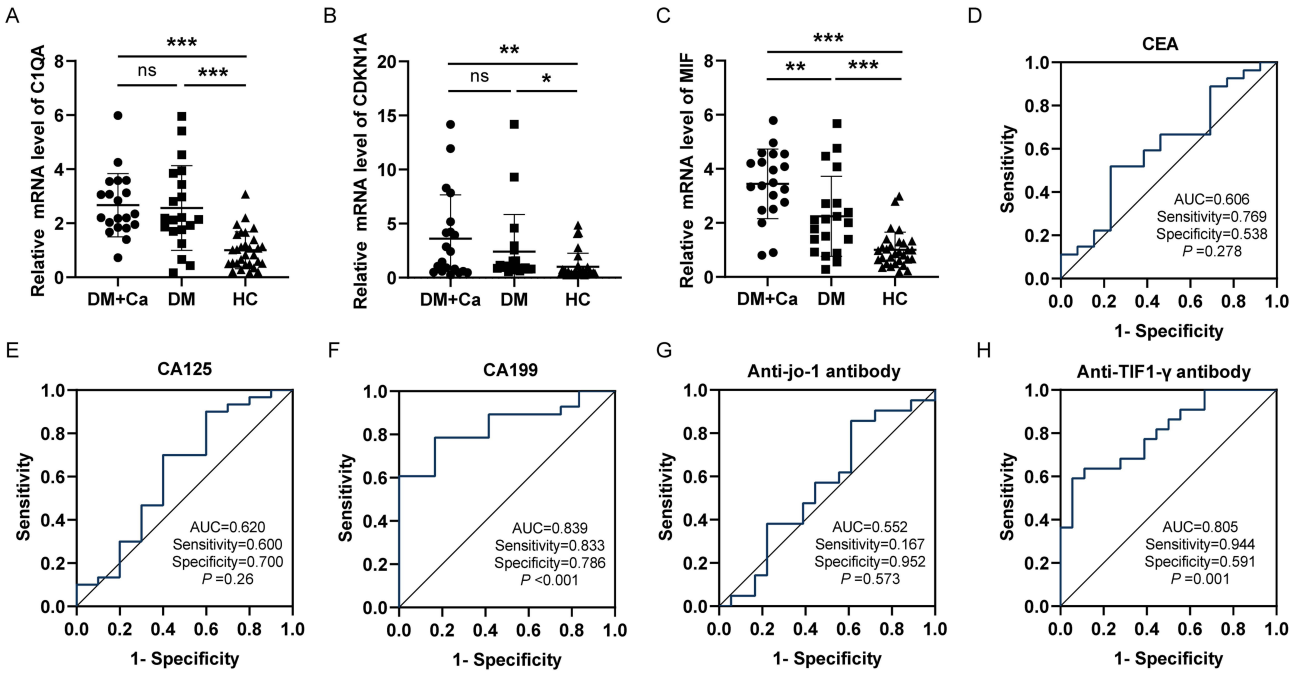

Figure 6 Expression level of the HUb gene, and ROC diagrams. (**A-C**) Differential expression of C1QA, CDKN1A,MIF in DM+Ca, DM and groups. (**D-H**) Receiver operating characteristic (ROC) of differentially expressed MIF mRNA between tumor-related indicators and positive and negative Anti-TIF1-Y antibodies. * P < 0.05, ** P < 0.01, *** P < 0.001, ns, the difference was not statistically significant.

the GEPIA dataset to analyze the MIF expression levels comprehensively via the interactive BodyMap. The median expression levels of MIF were different in most human tumor tissues and corresponding normal tissues, including brain, blood, lung, esophagus, pancreas, stomach, gallbladder, kidney, and thyroid gland. Notably, in the eye, neck, lymphoid tissues, and abdomen, MIF is expressed only in tumor tissues (Figure 7B). The expression levels of MIF in 33 tumors and

Table 2 Clinical and Laboratory Data of Subjects Studied

Laboratory Indexes	DM+ca(n=20)	DM(n=20)	HC(n=30)	$Z/F/x^2$	P
CRP(mg/L)[$M(Q_1, Q_3)$]	21.25±14.68	26.40±15.37	–	1.08	0.286
WBC(×10^9/L)(x±s)	4.29(1.25,8.90)	1.24(0.57,6.02)	–	−1.41	0.159
GR(×10^9/L)(x±s)	7.83±4.73	7.40±4.94	7.09±1.19	0.24	0.79
LY(×10^9/L)(x±s)	7.07±5.00	7.03±5.21	5.93±1.36	0.69	0.504
MO(×10^9/L)(x±s)	1.52±1.46	1.43±0.90	1.79±0.55	0.91	0.408
AST(U/L)(x±s)	0.45±0.24	0.47±0.26	0.37±0.09	1.98	0.146
ALT(U/L)(x±s)	29.15±14.46	26.15±9.94	28.53±6.27	0.50	0.611
ALB(g/L)(x±s)	31.45±20.24	34.40±30.43	34.20±7.84	0.14	0.868
Urea(mmol/L)(x±s)	35.00±5.59[ab]	41.5±7.58[b]	47.88±2.26	36.77	<0.001
Crea(umol/L)(x±s)	6.23±3.54	6.19±1.52	5.77±1.43	0.33	0.723
LDH(U/L)(x±s)	60.47±17.57	59.88±18.78	61.63±9.72	0.09	0.916
HBDH(U/L)(x±s)	277.8±143.00	252.70±80.86	–	0.68	0.50
CK(U/L)[$M(Q_1, Q_3)$]	196.7±34.42	198.1±60.26	–	0.09	0.929
CK-MB(U/L)(x±s)	143.5(32.25,200.80)	125.5(39.25,172.50)	-	−0.27	0.787
CEA[number(%)]	19.85±12.69	18.87±8.85	-	0.28	0.779
CA125[number(%)]	12(60)	1(5)	-	11.40	0.001
CA199[number(%)]	10(50)	0(0)	-	-	<0.001

(*Continued*)

Table 2 (Continued).

Laboratory Indexes	DM+ca(n=20)	DM(n=20)	HC(n=30)	$Z/F/x^2$	P
Anti-jo-1 antibody [number(%)]	10(50)	2(10)	-	5.83	0.016
Anti-TIF1-γ antibody [number(%)]	10(50)	8(40)	-	0.40	0.525
CRP(mg/L)[$M(Q_1, Q_3)$]	11(55)	7(35)	-	1.62	0.204

Abbreviations: ESR, erythrocyte sedimentation rates; CRP, c-reactive protein; WBC, white blood cell counts; GR, Neutrophil counts; LY, Lymphocyte; MO, Monocyte; AST, Aspartate aminotransferase; ALT, Alanine aminotransferase; ALB, albumin; Crea, serum creatinine; LDH, Lactate dehydrogenase; HBDH, alpha-hydroxybutyric dehydrogenase; CK, creatine kinase; CK-MB, Creatine Kinase Isoenzyme; CEA, carcino-embryonic antigen; CA125,Carbohydrate antigen 125; CA199,Carbohydrate antigen 199; [a] $P < 0.05$ (in comparison with the DM group); [b] $P < 0.05$ (in comparison with the HC group).

their corresponding normal tissues were also studied. The median expression of MIF was higher in BLCA, BRCA, CESC, COAD, DLBC, HNSC, KIRC, LUAD, LUSC, OV, PAAD, READ, SKCM, STAD, TGCT, THYM, UCEC, and UCS and lower in LAML (Figure 7C). A comparison of the two databases revealed that the expression levels of MIF

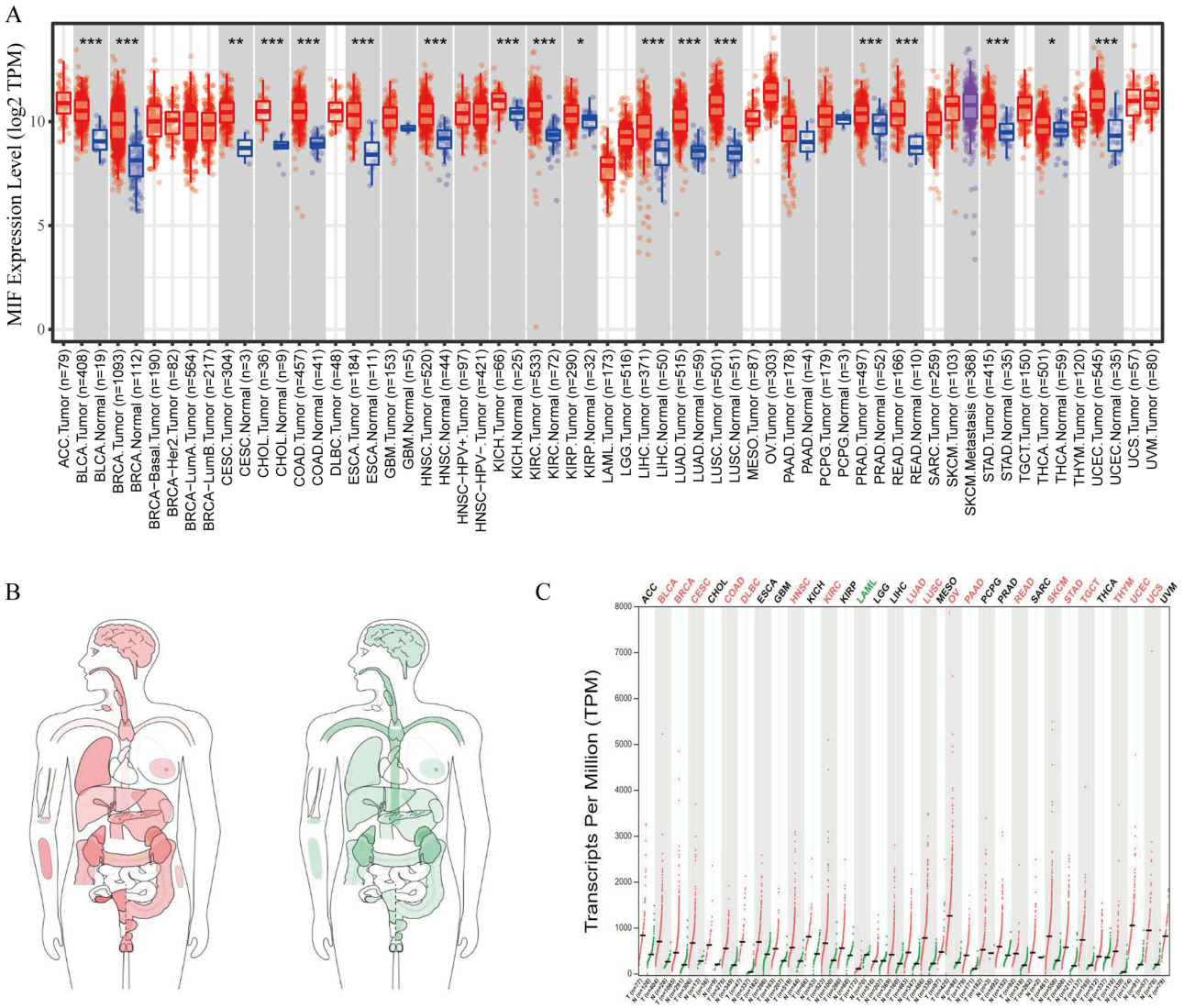

Figure 7 MIF mRNA expression profile in pan-cancer. (**A**) Levels of MIF expression in different cancer types from the TCGA cancer data set. Red, patients with high gene expression, blue, patients with low gene expression, purple, Expression characteristics of samples and interactions between high and low expression groups. *P < 0.05, * * P < 0.01, * * * P < 0.001. (**B**) Interactive BodyMap. (**C**) Dot pot, analysis of differences in MIF expression between tumor and normal samples from GEPIA. Each point represents the expression of the sample.

were approximately the same except for those of DLBC, LAML and LGG, which did not match those of normal tissues in TCGA.

Expression of MIF and the Prognosis of Cancer Patients

Cox regression analysis and Kaplan–Meier survival curves were used to evaluate the relationship between MIF expression and patient survival across cancers. The prognostic factors for OS were analyzed. Cox regression analysis of 33 cancer outcomes revealed that MIF expression was significantly associated with OS in patients with ACC, HNSC, LAML, LUAD, PCPG and UVM ($p < 0.05$) (Figure 8A). Kaplan–Meier revealed that higher MIF expression in ACC, CESC, LUAD, UVM, SARC and STAD patients was associated with poorer OS, whereas higher MIF expression in OV patients was associated with a better prognosis (Figure 8B). Neither the overexpression nor the underexpression of MIF in other tumors significantly affected OS ($P > 0.05$).

MIF Expression is Correlated with Immunomodulatory Genes, the TMB and MSI

Spearman correlation analysis revealed an association between MIF expression and the expression of immunomodulators (including immunoinhibitors, immunostimulators, and MHC molecules) across cancers. Among immunoinhibitors, MIF was positively correlated with ADORA2A, LAG3, LGALS9, PDCD1, PVRL2, and TGFB1 in most tumors and negatively correlated with other proteins (Figure 9A). In terms of immunostimulators, CD276 and TNFRSF 4/9/14/18/25 were positively correlated with most tumors and negatively correlated with the rest (Figure 9B). With regard to MHC molecules, we detected a positive correlation between HLA-A/B/C/F/G and TAPBP in most tumors and a roughly negative correlation with the other molecules (Figure 9C). To understand the role of MIF in predicting the efficacy of immune checkpoint inhibitor (ICI) therapy, we assessed the correlation between MIF expression and two well-known immunotherapy predictive biomarkers (34, 35), TMB and MSI. The results revealed that the expression of MIF in ACC, BLCA, BRCA, HNSC, LGG, LUAD, LUSC, PAAD, SKCM, STAD, UCEC, and UCS was positively correlated with TMB and negatively correlated with LAML and PCPG (Figure 9D). In addition, the expression of MIF and MSI in BRCA, CESC, COAD, DLBC, HNSC, KIRC, KIRP, LUSC, PRAD, SARC, CM, STAD and THCA was positively correlated, where as BLCA and READ were negatively correlated (Figure 9E). Our results suggest that MIF may affect the efficacy of ICIs in corresponding cancers.

Discussion

DM is a heterogeneous inflammatory myopathy. In recent years, the close relationship between DM and cancer risk has been widely recognized. The relationships between DM and cancer may include post-DM cancer, co-occurrence of DM and cancer, and postcancer DM. An increasing number of studies have reported a link between DM and cancer. However, to date, the molecular mechanism underlying the relationship between DM and cancer has rarely been reported. Therefore, we synthesized bioinformatics data to analyze and verify the characteristic genes involved in DM and to explore their differential expression, survival, immune infiltration and other variables. The aim of this study was to understand the pathogenesis of DM and cancer and provide a new starting point for clinicians to identify and treat DM patients with cancer.

In this study, we screened 321 DEGs and identified 216 upregulated genes and 105 downregulated genes. Subsequent GO enrichment analysis revealed that all DEGs were associated with congenital immunity, the type I interferon pathway, MHC protein complexes and cytokine activity, whereas KEGG enrichment analysis revealed associations with immune inflammatory and infectious signaling pathways. GO enrichment analysis revealed associations with infection, autoimmune disease, lymphatic disease, hematopoietic disease, and cancer. WGCNA revealed 15 modules and 399 trait-related genes. LASSO regression analysis and REF-SVM identified 3 hub genes, and the datasets were subsequently validated to confirm that MIF, C1QA and CDKN1A were highly expressed in DM. The 3 hub genes are valuable in the biological diagnosis of DM.

Macrophage migration inhibitor (MIF) is an inflammatory cytokine encoded within a functional polymorphic gene locus. On the one hand, MIF is a key upstream mediator in the host's congenital and adaptive immune and survival pathways, leading to the clearance of pathogens and thus protection from infectious disease. On the other hand, MIF is

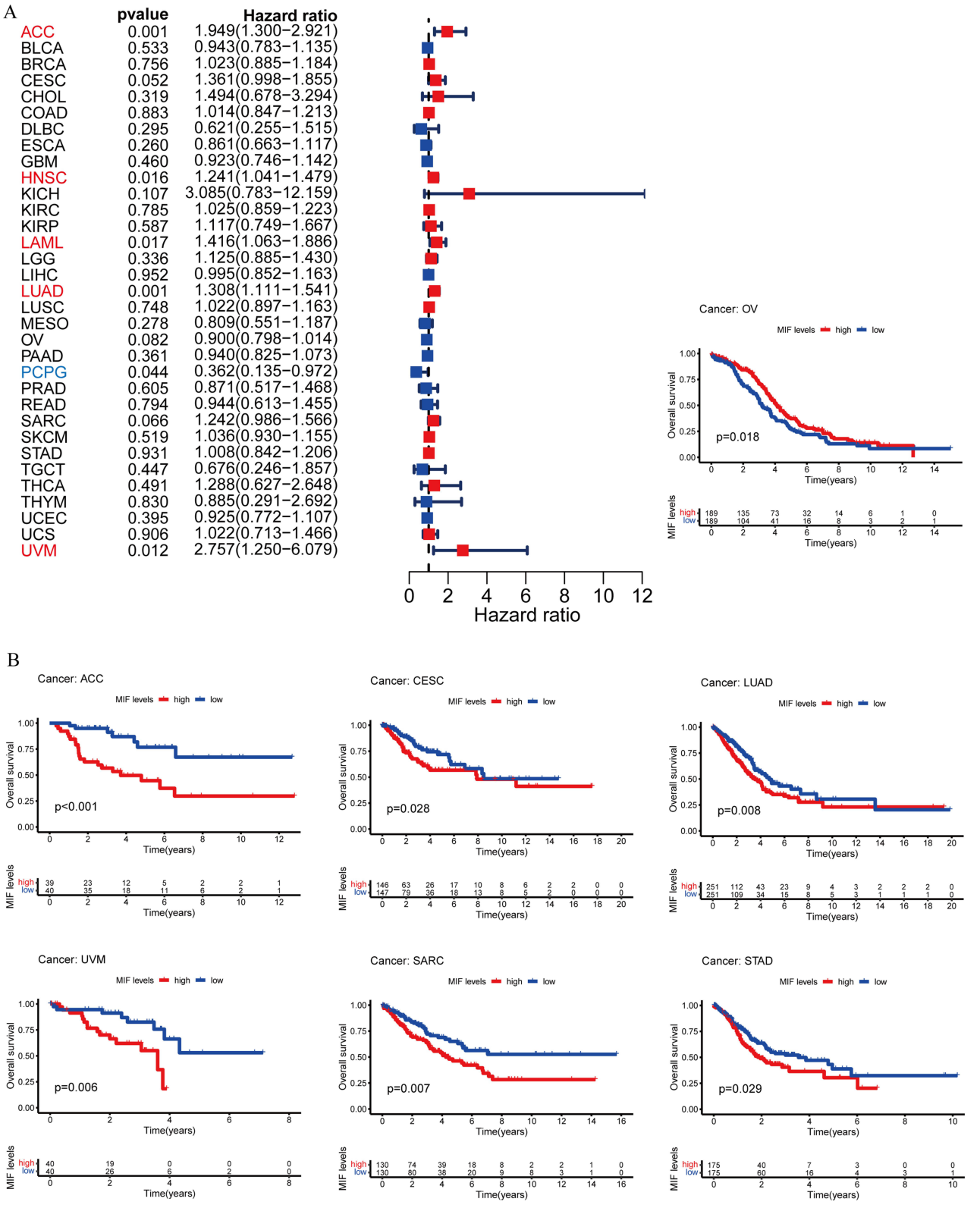

Figure 8 Correlation between MIF expression and prognosis in cancer patients. (**A**) Forest maps of MIF risk ratios for 33 tumors. (**B**) Kaplan-Meier survival curves for OS of patients with stratified MIF expression in ACC, HNSC, LAML, LUAD, PCPG, UVM and OV. Red, patients with high gene expression, blue, patients with low gene expression.

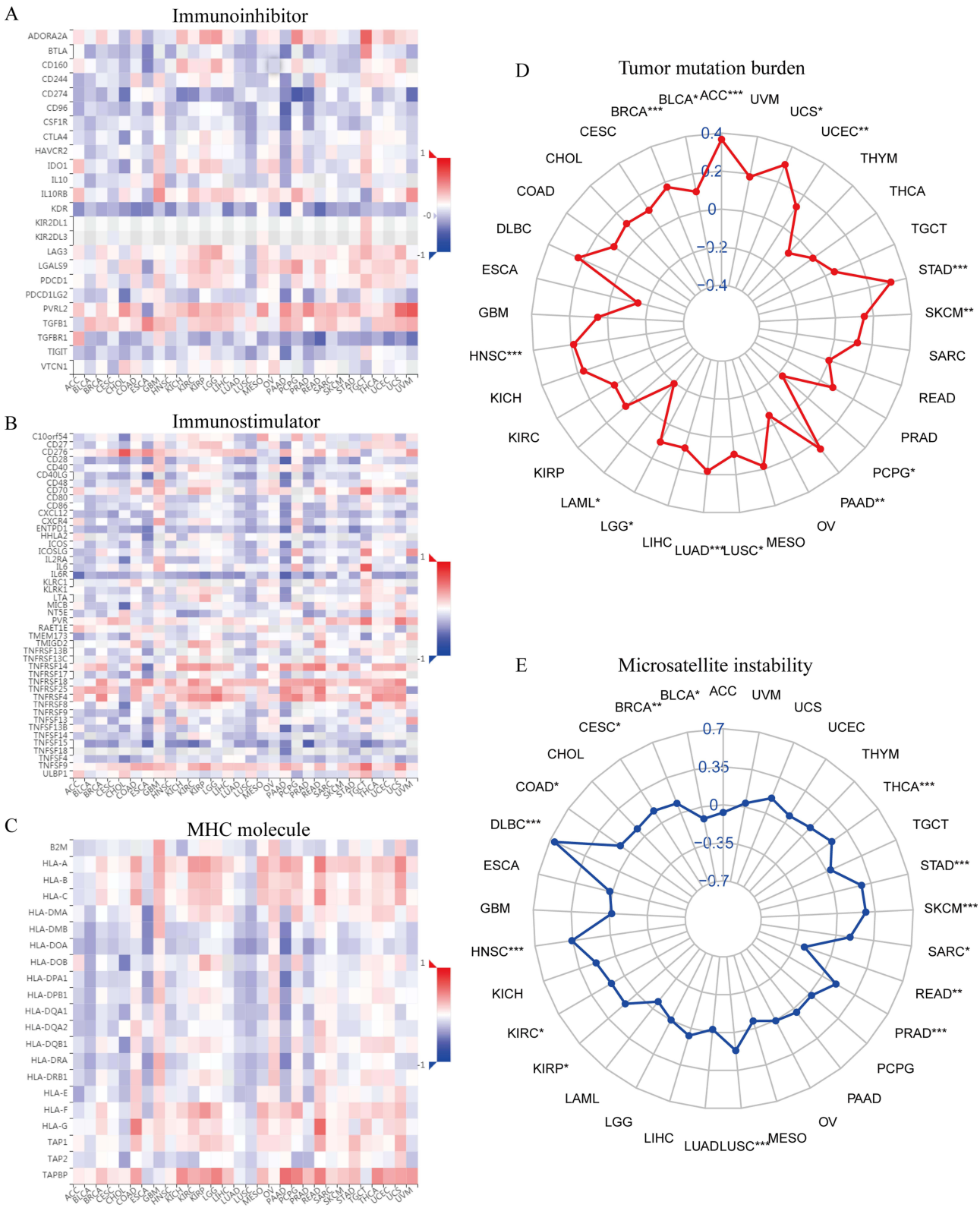

Figure 9 Correlation between MIF and immunomodulators, TMB and MSI in pan-cancer. (**A**) Immunoinhibitor. (**B**) Immunostimulator. (**C**) MHC molecule. (**D**) TMB. (**E**) MSI. * P < 0.05, ** P < 0.01, *** P < 0.001.

thought to be a skeletal muscle cytokine that may have functions beyond inflammatory pathology in complex regeneration responses to muscle fiber injury.[41] Corinna Preuße et al reported a significant increase in mRNA levels in patients with MIF compared with controls but no significant increase in aDM skeletal muscle tissue.[42] In their ELISA analysis, Jens Reimann et al confirmed that MIF protein expression was elevated in inflammatory myopathy.[43] The results revealed that the tissue concentrations increased only in the PM but not in the DM. Similarly, we used GSE128470 and GSE1551 chip data to confirm that MIF mRNA levels are elevated, and although these findings appear to be controversial, the exact role of MIF in DM patients is positive. Notably, MIF, as an immunomodulator, accelerates harmful inflammation and promotes cancer metastasis and progression, thereby exacerbating the disease.[44] The complement 1Q subcomponent A chain (C1QA) is a starting factor in the classical pathway of complement cascades.[45] C1q can identify various ligands and pathogens by modulating congenital immunity.[46] For example, impaired complement signaling may bias immunity toward more proinflammatory responses, resulting in increased inflammation and immune responsiveness in autoimmune diseases.[45,47] Notably, DM is associated with complement-mediated intramuscular microangiopathy, resulting in capillary loss, muscle ischemia, muscle fiber necrosis, and perifascial atrophy.[48,49] In addition, patients with DM have an excessive IFN-1 immune response,[22,50] and studies have shown a close functional link between complement and IFN-γ.[51–53] It is undeniable that C1QA may play a significant role in DM, although there is no direct evidence of its association with DM. Cyclin-dependent kinase inhibitor 1A (CDKN1A) is also known as p21. It is involved in cell cycle regulation (including stem cell proliferation), transcription, apoptosis, DNA repair and cell movement.[54,55] Le Wang et al reported a comprehensive bioinformatics approach involving CDKN1A that may regulate the development of DM through autophagic pathways.[56] CDKN1A is associated with other autoimmune diseases, such as systemic lupus erythematosus,[57] rheumatoid arthritis,[58] and Sjogren's syndrome.[59] However, there is no further evidence of CDKN1A in DM studies.

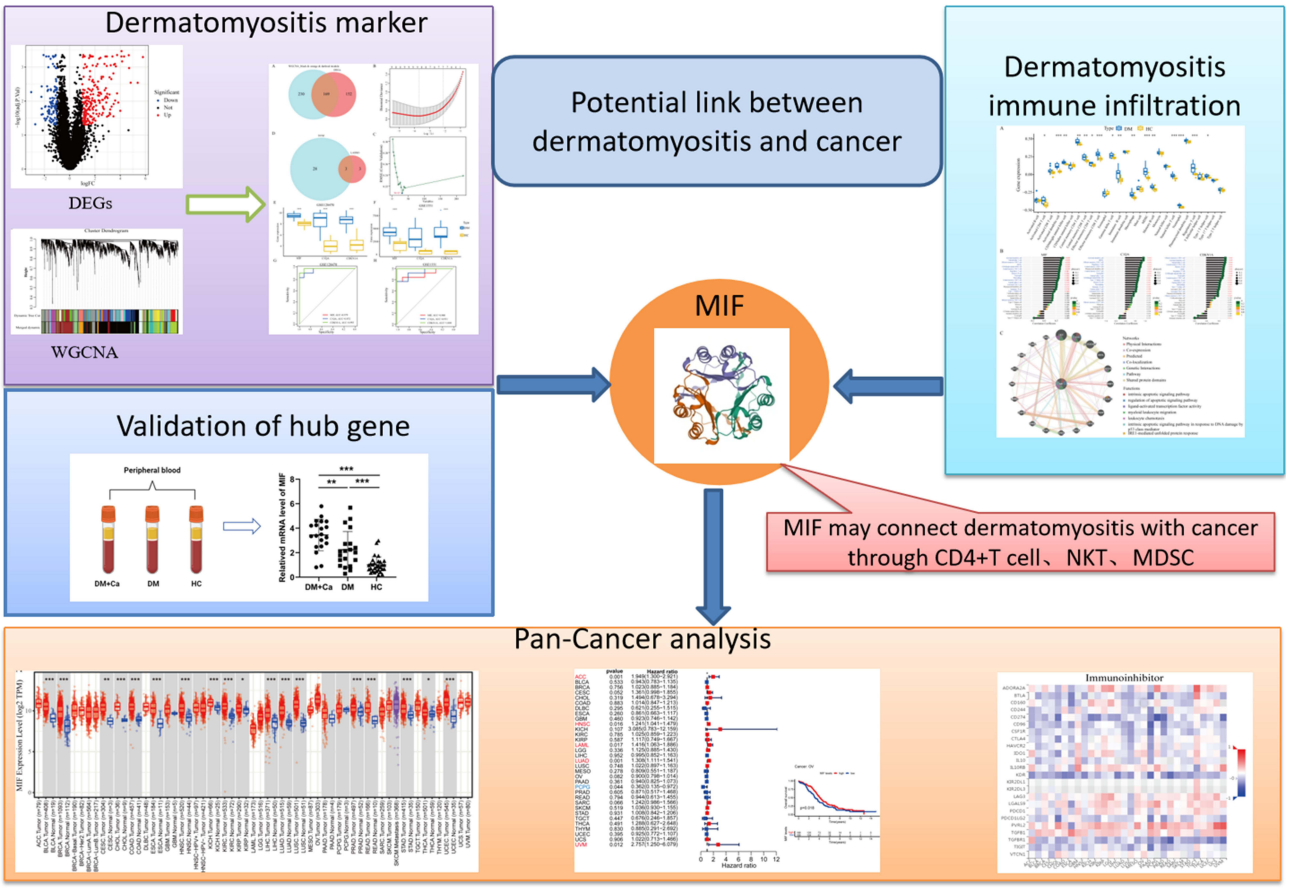

Figure 10 The study pipeline of our study.

Further immune infiltration analysis revealed that the numbers of T cells, B cells, NK cells, monocytes, macrophages, MDSCs, and neutrophils were higher in DM patients than in HCs. These results suggest that microenvironment regulation plays an important role in DM. In addition, MIF, C1QA and CDKN1A are strongly correlated with most of the differential immune cells. Therefore, we found that MIF is overexpressed in many cancers, and the data from GeneMANIA also suggested that MIF is involved in cancer regulation. A growing body of research supports the idea that MIF is directly related to cancer growth and development.[60] In addition, PCR was used to verify the expression level of MIF mRNA in the HC, DM and DM+Ca groups, and the data showed that the MIF mRNA level was significantly higher in the DM+Ca group than in the DM or HC group and higher in the DM group than in the HC group. ROC analysis also revealed that the MIF mRNA expression level was diagnostically significant for CA199 positivity (P<0.001, AUC=0.839) and anti-TIF1-Y antibody positivity (P=0.001, AUC=0.806). Therefore, we further investigated the role of MIF across cancers.

We also evaluated the prognostic significance of MIF for overall survival (OS) across cancers. Univariate Cox regression analysis revealed that the expression level of MIF was a risk factor for ACC, HNSC, LAML, LUAD and UVM and was also a protective factor for PCPG. The Kaplan–Meier survival curve revealed that MIF was a risk factor for ACC, CESC, LUAD, UVM, SARC, and STAD and was a protective factor in OV patients. Like in previous studies, patients with high MIF expression had poor outcomes in HNSC,[61] LAML,[62] LUAD,[63] UVM,[64] CESC,[65] SARC[66] and STAD.[67] Importantly, studies have shown that MIF is a risk factor for O**V**,[68] which is different from our results; OS as the endpoint may reduce the viability of clinical studies and that deaths from noncancer causes may lead to unreal conditions. Together, these results suggest that high expression of MIF may contribute to the progression of most tumor types.

MIF is also described as a soluble immune cell-derived factor,[69] a key mediator in the pathogenesis of cancer and inflammatory diseases.[70] The role of MIF in DM and cancer is fascinating. On the basis of the above findings, we analyzed the relationship between MIF and immunomodulators. Only RVRL2, TGFB1, CD276, TNFRSF4\ 9\ 18\ 25, HLA-A\ B\ C and TAPBP were positively correlated. In addition, we evaluated the relationships between MIF and TMB or MSI and found that the expression of MIF in ACC, BLCA, BRCA, HNSC, LGG, LUAD, LUSC, PAAD, SKCM, STAD, UCEC, UCS, LAML and PCPG was significantly related to TMB and that in BRCA, CESC, COAD, DLBC, HNSC, KIRC, KIRP, LUSC, PRAD, SKC, STIF and THCA, it was significantly related to MSI. Notably, in some studies, cancer was treated by altering the conformation of MIF[71] or developing MIF inhibitors.[72,73] Together, these findings suggest that MIF has great potential in future cancer research.

Limitations

This study has several limitations. First, the data available to us were limited, and only DM muscle tissue sequencing data were used for analysis. Second, although we performed human peripheral blood validation, the sample size was small, and we were unable to collect muscle tissue from DM patients and DM patients with cancer for analysis. Third, further prospective studies of DM patients with cancer should be undertaken to assess the relationship between MIF and cancer.

Conclusion

The study pipeline of our study is shown in Figure 10. The discovery of three central genes (MIF, C1QA and CDKN1A) will broaden our understanding of the molecular mechanism of DM. Further analysis of MIF revealed that MIF plays an important role in many types of cancer. In addition, MIF may interact with DM and 33 kinds of tumors through CD4+ Th1 cells, NKT cells and MDSC immunization, which will help clinicians improve experimental platforms to increase our understanding of and treatment strategies for DM patients with cancer.

Abbreviation

ACC, Adrenocortical carcinoma; BLCA, Bladder Urothelial Carcinoma; Breast invasive carcinoma; CESC, Cervical squamous cell carcinoma and endocervical adenocarcinoma; CHOL, Cholangiocarcinoma; COAD, Colon adenocarcinoma; DLBC, Lymphoid Neoplasm Diffuse Large B-cell Lymphoma; ESCA, Esophageal carcinoma; HNSC, Head and Neck squamous cell carcinoma; KICH, Kidney Chromophobe; KIRC, Kidney renal clear cell carcinoma; KIRP, Kidney renal papillary cell

carcinoma; LAML, Acute Myeloid Leukemia; LGG, Brain Lower Grade Glioma; LUAD, Lung adenocarcinoma; LUSC, Lung squamous cell carcinoma; OV, Ovarian serous cystadenocarcinoma; PAAD, Pancreatic adenocarcinoma; PCPG, Pheochromocytoma and Paraganglioma; PRAD, Prostate adenocarcinoma; READ, Rectum adenocarcinoma; SARC, Sarcoma; STAD, Stomach adenocarcinoma; SKCM, Skin Cutaneous Melanoma; TGCT, Testicular Germ Cell Tumors; THCA, Thyroid carcinoma; THYM, Thymoma; UCEC, Uterine Corpus Endometrial Carcinoma; UCS, Uterine Carcinosarcoma; UVM, Uveal Melanoma.

Data Sharing Statement

GSE128470 and GSE1551 datasets analysed during the current study are available in the [Gene Expression Omnibus] repository, [https://www.ncbi.nlm.nih.gov/geo/query/acc.cgi?acc=GSE128470, https://www.ncbi.nlm.nih.gov/geo/query/acc.cgi]. 33 cancers and normal tissues in The Cancer Genome Atlas (TCGA) datasets analysed during the current study are available in the [UCSC Xena] repository, [https://xenabrowser.net/datafiles/].

Ethics Approval and Consent to Participate

The studies involving human participants were reviewed and approved by the Ethics Committee of the Affiliated Hospital of North Sichuan Medical College (No. 2022ER575-1) and were conducted in accordance with the ethical norms of the 1975 helsinki Declaration. All participants provided informed consent to participate in this study.

Funding

This work was supported by funding from the National Natural Science Foundation of China (grant numbers 81974250); Science and Technology Project of Nanchong City (grant numbers 20SXCXTD0002, 20SXQT0308).

Disclosure

Jianwei Guo and Tianyi Lei contributed equally to this work and share first authorship. The authors declare no conflicts of interest. The funders had no role in the design of the study; in the collection, analyses, or interpretation of data; in the writing of the manuscript; or in the decision to publish the results.

References

1. Bohan A, Peter JB. Polymyositis and dermatomyositis (first of two parts). *N Engl J Med*. 1975;292(7):344–347. doi:10.1056/NEJM197502132920706
2. Bogdanov I, Kazandjieva J, Darlenski R, et al. Dermatomyositis: current concepts. *Clin Dermatol*. 2018;36(4):450–458. doi:10.1016/j.clindermatol.2018.04.003
3. Meyer A, Meyer N, Schaeffer M, et al. Incidence and prevalence of inflammatory myopathies: a systematic review. *Rheumatology (Oxford)*. 2015;54(1):50–63. doi:10.1093/rheumatology/keu289
4. DeWane ME, Waldman R, Lu J, et al. Dermatomyositis: clinical features and pathogenesis. *J Am Acad Dermatol*. 2020;82(2):267–281. doi:10.1016/j.jaad.2019.06.1309
5. Callen JP. Dermatomyositis. *Lancet*. 2000;355(9197):53–57. doi:10.1016/S0140-6736(99)05157-0
6. Bray F, Ferlay J, Soerjomataram I, et al. Global cancer statistics 2018: GLOBOCAN estimates of incidence and mortality worldwide for 36 cancers in 185 countries. *CA Cancer J Clin*. 2018;68(6):394–424. doi:10.3322/caac.21492
7. Hill CL, Zhang Y, Sigurgeirsson B, et al. Frequency of specific cancer types in dermatomyositis and polymyositis: a population-based study. *Lancet*. 2001;357(9250):96–100. doi:10.1016/S0140-6736(00)03540-6
8. Liu WC, Ho M, Koh W-P, et al. An 11-year review of dermatomyositis in Asian patients. *Ann Acad Med Singap*. 2010;39(11):843–847. doi:10.47102/annals-acadmedsg.V39N11p843
9. András C, Ponyi A, Constantin T, et al. Dermatomyositis and polymyositis associated with malignancy: a 21-year retrospective study. *J Rheumatol*. 2008;35(3):438–444.
10. Buchbinder R, Forbes A, Hall S, et al. Incidence of malignant disease in biopsy-proven inflammatory myopathy. A population-based cohort study. *Ann Intern Med*. 2001;134(12):1087–1095. doi:10.7326/0003-4819-134-12-200106190-00008
11. Buchbinder R, Hill CL. Malignancy in patients with inflammatory myopathy. *Curr Rheumatol Rep*. 2002;4(5):415–426. doi:10.1007/s11926-002-0087-9
12. Motomura K, Yamashita H, Yamada S, et al. Clinical characteristics and prognosis of polymyositis and dermatomyositis associated with malignancy: a 25-year retrospective study. *Rheumatol Int*. 2019;39(10):1733–1739. doi:10.1007/s00296-019-04428-z
13. Chen DY, Chen Y-M, Lan J-L, et al. Polymyositis/dermatomyositis and nasopharyngeal carcinoma: the Epstein-Barr virus connection? *J Clin Virol*. 2010;49(4):290–295. doi:10.1016/j.jcv.2010.08.015
14. Yang Z, Lin F, Qin B, et al. Polymyositis/dermatomyositis and malignancy risk: a metaanalysis study. *J Rheumatol*. 2015;42(2):282–291. doi:10.3899/jrheum.140566

15. Qiang JK, Kim WB, Baibergenova A, et al. Risk of malignancy in dermatomyositis and polymyositis. *J Cutan Med Surg*. 2017;21(2):131–136. doi:10.1177/1203475416665601
16. Fu T, Dai L-J, Wu S-Y, et al. Spatial architecture of the immune microenvironment orchestrates tumor immunity and therapeutic response. *J Hematol Oncol*. 2021;14(1):98. doi:10.1186/s13045-021-01103-4
17. de Visser KE, Eichten A, Coussens LM, et al. Paradoxical roles of the immune system during cancer development. *Nat Rev Cancer*. 2006;6 (1):24–37. doi:10.1038/nrc1782
18. Coussens LM, Zitvogel L, Palucka AK, et al. Neutralizing tumor-promoting chronic inflammation: a magic bullet? *Science*. 2013;339 (6117):286–291. doi:10.1126/science.1232227
19. Grivennikov SI, Greten FR, Karin M, et al. Immunity, inflammation, and cancer. *Cell*. 2010;140(6):883–899. doi:10.1016/j.cell.2010.01.025
20. Hanahan D, Weinberg R. Hallmarks of cancer: the next generation. *Cell*. 2011;144(5):646–674. doi:10.1016/j.cell.2011.02.013
21. Greenberg SA, Pinkus JL, Kong SW, et al. Highly differentiated cytotoxic T cells in inclusion body myositis. *Brain*. 2019;142(9):2590–2604. doi:10.1093/brain/awz207
22. Greenberg SA, Pinkus JL, Pinkus GS, et al. Interferon-alpha/beta-mediated innate immune mechanisms in dermatomyositis. *Ann Neurol*. 2005;57 (5):664–678. doi:10.1002/ana.20464
23. Ritchie ME, Phipson B, Wu D, et al. limma powers differential expression analyses for RNA-sequencing and microarray studies. *Nucleic Acids Res 43:e47*. 2015;43(7):e47–e47. doi:10.1093/nar/gkv007
24. Gene Ontology Consortium. The Gene Ontology (GO) project in 2006. *Nucleic Acids Res*. 2006;34(90001):D322–326. doi:10.1093/nar/gkj021
25. Kanehisa M, Goto S. KEGG: Kyoto Encyclopedia of Genes and Genomes. *Nucleic Acids Res*. 2000;28(1):27–30. doi:10.1093/nar/28.1.27
26. Yu G, Wang L-G, Yan G-R, et al. DOSE: an R/Bioconductor package for disease ontology semantic and enrichment analysis. *Bioinformatics*. 2015;31(4):608–609. doi:10.1093/bioinformatics/btu684
27. Zhang B, Horvath S. A general framework for weighted gene co-expression network analysis. *Stat Appl Genet Mol Biol 4:Article17*. 2005;4(1). doi:10.2202/1544-6115.1128.
28. Langfelder P, Horvath S. WGCNA: an R package for weighted correlation network analysis. *BMC Bioinformatics*. 2008;9(1):559. doi:10.1186/1471-2105-9-559
29. Jia A, Xu L, Wang Y, et al. Venn diagrams in bioinformatics. *Brief Bioinform*. 2021;22(5). doi:10.1093/bib/bbab108.
30. Huang ML, Hung Y-H, Lee WM, et al. SVM-RFE based feature selection and Taguchi parameters optimization for multiclass SVM classifier. *ScientificWorldJournal*. 2014;2014:795624. doi:10.1155/2014/795624
31. Yang R, Li H, Fu L, et al. An efficient approach to large-scale genotype-phenotype association analyses. *Brief Bioinform*. 2014;15(5):814–822. doi:10.1093/bib/bbt061
32. Robin X, Turck N, Hainard A, et al. pROC: an open-source package for R and S+ to analyze and compare ROC curves. *BMC Bioinformatics*. 2011;12(1):77. doi:10.1186/1471-2105-12-77
33. Hänzelmann S, Castelo R, Guinney J, et al. GSVA: gene set variation analysis for microarray and RNA-seq data. *BMC Bioinformatics*. 2013;14 (1):7. doi:10.1186/1471-2105-14-7
34. Charoentong P, Finotello F, Angelova M, et al. Pan-cancer immunogenomic analyses reveal genotype-immunophenotype relationships and predictors of response to checkpoint blockade. *Cell Rep*. 2017;18(1):248–262. doi:10.1016/j.celrep.2016.12.019
35. Franz M, Rodriguez H, Lopes C, et al. GeneMANIA update 2018. *Nucleic Acids Res*. 2018;46(W1):W60–w64. doi:10.1093/nar/gky311
36. Li T, Fu J, Zeng Z, et al. TIMER2.0 for analysis of tumor-infiltrating immune cells. *Nucleic Acids Res*. 2020;48(W1):W509–w514. doi:10.1093/nar/gkaa407
37. Tang Z, Kang B, Li C, et al. GEPIA2: an enhanced web server for large-scale expression profiling and interactive analysis. *Nucleic Acids Res 47: W556-w560*. 2019;47(W1):W556–W560. doi:10.1093/nar/gkz430
38. Ru B, Wong CN, Tong Y, et al. TISIDB: an integrated repository portal for tumor-immune system interactions. *Bioinformatics*. 2019;35 (20):4200–4202. doi:10.1093/bioinformatics/btz210
39. Jardim DL, Goodman A, de Melo Gagliato D, et al. The challenges of tumor mutational burden as an immunotherapy biomarker. *Cancer Cell*. 2021;39(2):154–173. doi:10.1016/j.ccell.2020.10.001
40. Baretti M, Le DT. DNA mismatch repair in cancer. *Pharmacol Ther*. 2018;189:45–62. doi:10.1016/j.pharmthera.2018.04.004
41. Ritter F, Franzeck F, Geisshardt J, et al. Gout arthritis during admission for decompensated heart failure-a descriptive analysis of risk factors, treatment and prognosis. *Front Med (Lausanne)*. 2022;9:789414. doi:10.3389/fmed.2022.789414
42. Preuße C, Allenbach Y, Hoffmann O, et al. Differential roles of hypoxia and innate immunity in juvenile and adult dermatomyositis. *Acta Neuropathol Commun*. 2016;4(1):45. doi:10.1186/s40478-016-0308-5
43. Reimann J, Schnell S, Schwartz S, et al. Macrophage migration inhibitory factor in normal human skeletal muscle and inflammatory myopathies. *J Neuropathol Exp Neurol*. 2010;69(6):654–662. doi:10.1097/NEN.0b013e3181e10925
44. Sumaiya K, Langford D, Natarajaseenivasan K, et al. Macrophage migration inhibitory factor (MIF): a multifaceted cytokine regulated by genetic and physiological strategies. *Pharmacol Ther*. 2022;233:108024. doi:10.1016/j.pharmthera.2021.108024
45. Lu J, Kishore U. C1 complex: an adaptable proteolytic module for complement and non-complement functions. *Front Immunol*. 2017;8:592. doi:10.3389/fimmu.2017.00592
46. Mangogna A, Agostinis C, Bonazza D, et al. Is the Complement protein C1q a Pro- or anti-tumorigenic factor? Bioinformatics analysis involving human carcinomas. *Front Immunol*. 2019;10:865. doi:10.3389/fimmu.2019.00865
47. Lood C, Gullstrand B, Truedsson L, et al. C1q inhibits immune complex-induced interferon-alpha production in plasmacytoid dendritic cells: a novel link between C1q deficiency and systemic lupus erythematosus pathogenesis. *Arthritis Rheum*. 2009;60(10):3081–3090. doi:10.1002/art.24852
48. Lahoria R, Selcen D, Engel AG, et al. Microvascular alterations and the role of complement in dermatomyositis. *Brain*. 2016;139(7):1891–1903. doi:10.1093/brain/aww122
49. Kissel JT, Halterman RK, Rammohan KW, et al. The relationship of complement-mediated microvasculopathy to the histologic features and clinical duration of disease in dermatomyositis. *Arch Neurol*. 1991;48(1):26–30. doi:10.1001/archneur.1991.00530130034016
50. Wenzel J, Schmidt R, Proelss J, et al. Type I interferon-associated skin recruitment of CXCR3+ lymphocytes in dermatomyositis. *Clin Exp Dermatol*. 2006;31(4):576–582. doi:10.1111/j.1365-2230.2006.02150.x

51. Lalli PN, Strainic MG, Yang M, et al. Locally produced C5a binds to T cell-expressed C5aR to enhance effector T-cell expansion by limiting antigen-induced apoptosis. *Blood*. 2008;112(5):1759–1766. doi:10.1182/blood-2008-04-151068
52. Liu J, Miwa T, Hilliard B, et al. The complement inhibitory protein DAF (CD55) suppresses T cell immunity in vivo. *J Exp Med*. 2005;201 (4):567–577. doi:10.1084/jem.20040863
53. Strainic MG, Liu J, Huang D, et al. Locally produced complement fragments C5a and C3a provide both costimulatory and survival signals to naive CD4+ T cells. *Immunity*. 2008;28(3):425–435. doi:10.1016/j.immuni.2008.02.001
54. Ticli G, Cazzalini O, Stivala LA, et al. Revisiting the Function of p21(CDKN1A) in DNA repair: the influence of protein interactions and stability. *Int J Mol Sci*. 2022;23(13):7058. doi:10.3390/ijms23137058
55. Cazzalini O, Scovassi AI, Savio M, et al. Multiple roles of the cell cycle inhibitor p21(CDKN1A) in the DNA damage response. *Mutat Res*. 2010;704(1–3):12–20. doi:10.1016/j.mrrev.2010.01.009
56. Wang L, Fang D, Liu Y, et al. Autophagy-related genes are potential diagnostic biomarkers for dermatomyositis. *Ann Transl Med*. 2022;10(4):228. doi:10.21037/atm-22-70
57. Eghbalpour F, Aghaei M, Ebrahimi M, et al. Effect of indole-3-carbinol on transcriptional profiling of wound-healing genes in macrophages of systemic lupus erythematosus patients: an RNA sequencing assay. *Lupus*. 2020;29(8):954–963. doi:10.1177/0961203320929746
58. Gang X, Xu H, Si L, et al. Treatment effect of CDKN1A on rheumatoid arthritis by mediating proliferation and invasion of fibroblast-like synoviocytes cells. *Clin Exp Immunol*. 2018;194(2):220–230. doi:10.1111/cei.13161
59. de Paiva CS, Trujillo-Vargas CM, Schaefer L, et al. Differentially expressed gene pathways in the conjunctiva of Sjögren syndrome keratoconjunctivitis sicca. *Front Immunol*. 2021;12:702755. doi:10.3389/fimmu.2021.702755
60. Conroy H, Mawhinney L, Donnelly SC, et al. Inflammation and cancer: macrophage migration inhibitory factor (MIF)--The potential missing link. *Qjm*. 2010;103(11):831–836. doi:10.1093/qjmed/hcq148
61. Kindt N, Laurent G, Nonclercq D, et al. Pharmacological inhibition of macrophage migration inhibitory factor interferes with the proliferation and invasiveness of squamous carcinoma cells. *Int J Oncol*. 2013;43(1):185–193. doi:10.3892/ijo.2013.1944
62. Abdul-Aziz AM, Shafat MS, Mehta TK, et al. MIF-induced stromal PKCβ/IL8 is essential in human acute myeloid leukemia. *Cancer Res*. 2017;77 (2):303–311. doi:10.1158/0008-5472.CAN-16-1095
63. Jiang T, Yan Y, Zhou K, et al. Characterization of evolution trajectory and immune profiling of brain metastasis in lung adenocarcinoma. *NPJ Precis Oncol*. 2021;5(1):6. doi:10.1038/s41698-021-00151-w
64. Ambrosini G, Rai AJ, Carvajal RD, et al. Uveal melanoma exosomes induce a prometastatic microenvironment through macrophage migration inhibitory factor. *Mol Cancer Res*. 2022;20(4):661–669. doi:10.1158/1541-7786.MCR-21-0526
65. Xiao DZ, Dai B, Chen J, et al. Loss of macrophage migration inhibitory factor impairs the growth properties of human HeLa cervical cancer cells. *Cell Prolif*. 2011;44(6):582–590. doi:10.1111/j.1365-2184.2011.00787.x
66. Wang C, Zhou X, Li W, et al. Macrophage migration inhibitory factor promotes osteosarcoma growth and lung metastasis through activating the RAS/MAPK pathway. *Cancer Lett*. 2017;403:271–279. doi:10.1016/j.canlet.2017.06.011
67. He XX, Yang J, Ding YW, et al. Increased epithelial and serum expression of macrophage migration inhibitory factor (MIF) in gastric cancer: potential role of MIF in gastric carcinogenesis. *Gut*. 2006;55(6):797–802. doi:10.1136/gut.2005.078113
68. Agarwal R, Whang DH, Alvero AB, et al. Macrophage migration inhibitory factor expression in ovarian cancer. *Am J Obstet Gynecol*. 2007;196 (4):348.e341–345. doi:10.1016/j.ajog.2006.12.030
69. Bloom BR, Bennett B. Mechanism of a reaction in vitro associated with delayed-type hypersensitivity. *Science*. 1966;153(3731):80–82. doi:10.1126/science.153.3731.80
70. Kang I, Bucala R. The immunobiology of MIF: function, genetics and prospects for precision medicine. *Nat Rev Rheumatol*. 2019;15(7):427–437. doi:10.1038/s41584-019-0238-2
71. Schinagl A, Thiele M, Douillard P, et al. Oxidized macrophage migration inhibitory factor is a potential new tissue marker and drug target in cancer. *Oncotarget*. 2016;7(45):73486–73496. doi:10.18632/oncotarget.11970
72. Hussain F, Freissmuth M, Völkel D, et al. Human anti-macrophage migration inhibitory factor antibodies inhibit growth of human prostate cancer cells in vitro and in vivo. *Mol Cancer Ther*. 2013;12(7):1223–1234. doi:10.1158/1535-7163.MCT-12-0988
73. Xu L, Li Y, Sun H, et al. Current developments of macrophage migration inhibitory factor (MIF) inhibitors. *Drug Discov Today*. 2013;18 (11–12):592–600. doi:10.1016/j.drudis.2012.12.013